LITERATURE CITED

1. Weimer, R. F., and J. M. Prausnitz, *Hydrocarbon Process. Petrol. Refiner*, **44**, 237 (1965).
2. Scatchard, G., G. M. Wilson, and F. G. Satkiewicz, *J. Am. Chem. Soc.*, **86**, 125 (1964).
3. Hermsen, R. W., and J. M. Prausnitz, *Chem. Eng. Sci.*, **18**, 485 (1963).
4. Orye, R. V., and J. M. Prausnitz, *Trans. Faraday Soc.*, **61**, 1338 (1965).
5. Brown, I., and F. Smith, *Australian J. Chem.*, **10**, 423 (1957).
6. Barker, J. A., *ibid.*, **6**, 207 (1953).
7. Prausnitz, J. M., C. A. Eckert, R. V. Orye, and J. P. O'Connell, "Computer Calculations for Multicomponent Vapor-Liquid Equilibria," Prentice-Hall, Englewood Cliffs, N. J. (1967).
8. Anderson, R., R. Cambio, and J. M. Prausnitz, *AIChE J.*, **8**, 65 (1962).
9. Deal, C. H., and E. L. Derr, *Ind. Eng. Chem. Process Design Develop.*, **3**, 394 (1964).
10. Gerster, J. A., J. A. Gorton, and R. Eklund, *J. Chem. Eng. Data*, **5**, 423 (1960).

Manuscript received September 22, 1967; revision received November 6, 1967; paper accepted November 8, 1967.

Correlations for Adsorption of a Binary Gas Mixture on a Heterogeneous Adsorbent—the Methane-Ethane-Silica Gel System

SHIGEHIKO MASUKAWA and RIKI KOBAYASHI

William Marsh Rice University, Houston, Texas

Correlations for the adsorption of a binary gas mixture on a heterogeneous adsorbent have been developed for both mobile and immobile models. Experiments determined the form for the expression of the surface heterogeneity, and only one dimensionless constant for the molecular size was required.

The correlations were tested by experimental data on the system methane-ethane-silica gel. For the same amount of adsorption the root-mean-square deviation of calculated versus experimental fugacity ranged from 4.1 to 5.2% for methane and from 2.7 to 3.4% for ethane at 5.0, 15.0, 25.0, and 35.0°C. for surface coverage ranging from zero to monolayer and for the complete composition range. The system at these conditions is classified as highly mobile based on examination of spreading pressure curves, both experimental and calculated based on the correlations.

The effect of surface heterogeneity of the adsorbent on the adsorption isotherms of gases has been studied by several investigators (*4, 5, 7, 11, 13*). The theories cover localized (immobile) and mobile adsorption, with and without lateral interactions among the adsorbates. Surface heterogeneity is usually given in terms of the probability distribution of the adsorptive energy on the surface of the adsorbent. Some mathematical expressions used for the distribution of the adsorptive energy have been a step function (*4*), a truncated sine function (*4*), exponential functions (*2, 13*), Gaussian functions (*11, 13*), and a log-normal function (*7*). The mathematical expression for a specific gas-solid system and the amount of the lateral interaction energy among adsorbates with respect to the total adsorptive energy are difficult to determine.

An empirical determination of the distribution function was first attempted by Sips (*12*). He assumed a Freundlich type adsorption isotherm and then determined the resulting expression for the surface heterogeneity. Honig and Hill (*6*) followed Sips' approach but still assumed a particular form for the adsorption isotherm.

In this work an empirical determination of the distribution function of the adsorptive energy has been made without assuming a particular type of adsorption isotherm. The adsorptive energy, including the lateral interaction among adsorbates, is assumed to be a function only of the surface coverage at a constant temperature, although the form of the function is not known. Isothermal derivations for both mobile and immobile adsorption models for binary gas mixtures have been made. Experimental data required are fugacity versus the amount of adsorption for both pure components for the pure state and fugacity versus the amount of adsorption ratio for the infinite dilution of one component in the other. These data are easily obtained by a chromatographic method (*8, 9*). Experimental data on the system methane-ethane-silica gel have been used to check the correlations at ambient temperatures up to about monolayer adsorption.

Shigehiko Masukawa is at the University of Tokyo, Tokyo, Japan.

THEORETICAL MOBILE ADSORPTION

Fundamental Formulations

The derivation by Hill (*3*) for the isotherm for mobile adsorption of a pure component was based on a van der Waals type formulation. The adsorbed phase has been defined elsewhere (*8*). When modifications are made for the application to a binary gas mixture of different molecular sizes and for a three-dimensional expression in place of the two-dimensional expression, the resulting partition function of the adsorbates in a mobile model is

$$Q_m = \left[f_{m,1}^{N_1} f_{m,2}^{N_2} / (N_1!\, N_2!) \right] (V - b_1 N_1 - b_2 N_2)^{N_1+N_2} \exp\{[N_1 E_{m,1}(\theta_m) + N_2 E_{m,2}(\theta_m)]/(kT)\} \quad (1)$$

The surface coverage, θ, is defined by

$$\theta_m = (b_1 N_1 + b_2 N_2)/V \quad (2)$$

The chemical potential, μ, and the fugacity of a spe-

cies j are related to the partition function by

$$\mu_j/(kT) = \mu_j^o(T)/(kT) + \ln f_j = -\partial \ln Q_m/\partial N_j \quad (3)$$

The spreading pressure, π, of the adsorbed phase is defined as the conjugate intensive quantity of the surface area of the adsorbent. Therefore

$$\pi/(kT) = \partial \ln Q_m/\partial A = h\ \partial \ln Q_m/\partial V \quad (4)$$

Adsorptive Energy

From Equations (1), (2), and (3) the fugacities of the two components are given by

$$\begin{aligned}(\ln f_1)_m &= \ln N_1 - \ln (V - b_1 N_1 - b_2 N_2) \\ &+ b_1(N_1 + N_2)/(V - b_1 N_1 - b_2 N_2) \\ &- \{E_{m,1}(\theta_m) + (b_1/V)\,[N_1 E'_{m,1}(\theta_m) \\ &\qquad + N_2 E'_{m,2}(\theta_m)]\}/(kT) \\ &- \ln j_{m,1} - \mu_1^o(T)/(kT) \quad (5)\end{aligned}$$

$$\begin{aligned}(\ln f_2)_m &= \ln N_2 - \ln (V - b_1 N_1 - b_2 N_2) \\ &+ b_2 (N_1 + N_2)/(V - b_1 N_1 - b_2 N_2) \\ &- \{E_{m,2}(\theta_m) + (b_2/V)\,[N_1 E'_{m,1}(\theta_m) \\ &\qquad + N_2 E'_{m,2}(\theta_m)]\}/(kT) \\ &- \ln j_{m,2} - \mu_2^o(T)/(kT) \quad (6)\end{aligned}$$

An isothermal, composition independent, function of θ_m may be defined from Equations (5) and (6) as

$$\begin{aligned}\xi_m(\theta_m) &\equiv \ln (f_1 N_1) - (b_1/b_2) \ln (f_2/N_2) \\ &= [(b_1/b_2) - 1] \ln (1 - \theta_m) \\ &+ [(b_1/b_2)\, E_{m,2}(\theta_m) - E_{m,1}(\theta_m)]/(kT) \\ &+ [(b_1/b_2) - 1] \ln V + C_3 \quad (7)\end{aligned}$$

The $j_{m,j}$ and $\mu_j^o(T)$ terms are contained in C_3, which is assumed to be constant at isothermal conditions. Plots of the empirical grouping $[\ln(f_1/N_1) - (b_1/b_2) \ln (f_2/N_2)]$ vs. θ_m should, therefore, coincide to form a single curve when the ratio (b_1/b_2) is correctly chosen. A trial and error procedure is used on the ratio of the molecular volumes (b_1/b_2) until the plots converge. The function ξ_m is taken as the curve from which the plots give the smallest value of the root-mean-square deviation.

For the adsorption of the pure components Equations (5) and (6) reduce to

$$\begin{aligned}\ln(f_1^o/N_1^o)_m &= \\ &- \ln (V - b_1 N_1^o) + b_1 N_1^o/(V - b_1 N_1^o) \\ &- [E_{m,1}(\theta_m) + (b_1/V)\, N_1^o\, E'_{m,1}(\theta_m)]/(kT) \\ &- \ln j_{m,1} - \mu_1^o(T)/(kT) \quad (5a)\end{aligned}$$

$$\begin{aligned}\ln(f_2^o/N_2^o)_m &= \\ &- \ln (V - b_2 N_2^o) + b_2 N_2^o/(V - b_2 N_2^o) \\ &- [E_{m,2}(\theta_m) + (b_2/V)\, N_2^o\, E'_{m,2}(\theta_m)]/(kT) \\ &- \ln j_{m,2} - \mu_2^o(T)/(kT) \quad (6a)\end{aligned}$$

At constant coverage, $\theta_m = b_1 N_1^o/V = b_2 N_2^o/V$, and the difference of Equations (5a) and (6a) gives the function

$$\begin{aligned}\phi_m(\theta_m) &\equiv \ln (f_1^o/N_1^o)_m - \ln (f_2^o/N_2^o)_m \\ &= \{[E_{m,2}(\theta_m) - E_{m,1}(\theta_m)] \\ &+ \theta_m [E'_{m,2}(\theta_m) - E'_{m,1}(\theta_m)]\}/(kT) + C_4 \quad (8)\end{aligned}$$

The experimental data determines the functions $\xi_m(\theta_m)$ and $\phi_m(\theta_m)$. Therefore, the average adsorptive energies E may be solved. Equation (8) is a differential equation of $\{[E_{m,2}(\theta_m) - E_{m,1}(\theta_m)]/(kT)\}$ with respect to θ_m, which may be solved to give

$$\begin{aligned}\psi_m(\theta_m) &\equiv [E_{m,2}(\theta_m) - E_{m,1}(\theta_m)]/(kT) \\ &= (1/\theta_m) \int [\phi_m(\theta_m) - C_4]\ d\theta_m \quad (9)\end{aligned}$$

The initial condition $\psi_m(0) =$ finite was used.

Equations (7) and (9) can be solved simultaneously for the surface heterogeneity; that is, the average adsorptive energy E

$$\begin{aligned}E_{m,1}(\theta_m)/(kT) &= [b_1\, \psi_m(\theta_m) - b_2\, \xi_m(\theta_m)]/(b_2 - b_1) \\ &- \ln (1 - \theta_m) + C_5 \quad (10)\end{aligned}$$

$$\begin{aligned}E_{m,2}(\theta_m)/(kT) &= b_2\, [\psi_m(\theta_m) - \xi_m(\theta_m)]/(b_2 - b_1) \\ &- \ln (1 - \theta_m) + C_5 \quad (11)\end{aligned}$$

Correlation

The insertion of Equations (10) and (11) into Equations (5), (5a), (6), and (6a) and rearrangement at the restriction of constant coverage leads to the simple relations

$$[\ln (f_1/N_1) - \ln (f_1^o/N_1^o)]_m = -(b_2/V)\, N_2\, \xi'_m(\theta_m) \quad (12)$$

$$[\ln (f_2/N_2) - \ln (f_2^o/N_2^o)]_m = +(b_2/V)\, N_1\, \xi'_m(\theta_m) \quad (13)$$

By introducing the definitions

$$N_m^* = N_1 + (b_2/b_1)\, N_2 = (V/b_1)\, \theta_m \quad (14)$$

$$\Xi_m(N_m^*/A) = \xi_m(\theta_m) \quad (15)$$

Alternative forms for Equations (12) and (13) are obtained

$$\begin{aligned}&[\ln (f_1/N_1) - \ln (f_1^o/N_1^o)]_m = \\ &\qquad -(b_2/b_1)\, (N_2/A)\, \Xi'_m(N_m^*/A) \quad (12a)\end{aligned}$$

$$\begin{aligned}&[\ln (f_2/N_2) - \ln (f_2^o/N_2^o)]_m = \\ &\qquad +(b_2/b_1)\, (N_1/A)\, \Xi'_m(N_m^*/A) \quad (13a)\end{aligned}$$

When the pure component isotherms are known, the mixture isotherms can be calculated from Equations (12a) and (13a), where the ratio (b_1/b_2) and the function $\Xi_m(N_m^*/A)$ are determined empirically by the procedure given below Equation (7). The correlations in Equations (12a) and (13a) are suitable for the calculation of fugacities corresponding to a fixed amount of adsorption.

IMMOBILE ADSORPTION

Fundamental Formulations

The following derivation for the isotherm for immobile adsorption is based on the formulation by Hill (4) for a pure component. Modifications have been introduced for a binary gas mixture of two different molecular sizes which, therefore, cover different areas of the adsorbent per adsorbed molecule. The distribution of the chain links of a molecule (for example, ethane is two; propane is three methyl links) on the adsorption surface is similar to the case of a polymer molecule in a liquid (1).

The resulting partition function of the adsorbates in an immobile model is

$$Q_i = \left[\left(\prod_j^{N_1 N_2} \prod_k w_{jk} \right) \Big/ (N_1!\, N_2!) \right] j_{i,1}^{N_1}\, j_{1,2}^{N_2}$$

$$\exp\{[N_1\ E_{i,1}(\theta_i) + N_2\ E_{i,2}(\theta_i)]/(kT)\} \quad (16)$$

The surface coverage, θ_i, is defined by

$$\theta_i = (m_1\ N_1 + m_2\ N_2)/M \quad (17)$$

It is shown that

$$\ln\left(\prod_j^{N_1} \prod_k^{N_2} w_{jk}\right)$$
$$= \ln M! - \ln (M - m_1\ N_1 - m_2\ N_2)!$$
$$+ (N_1 + N_2) \ln c$$
$$+ [N_1\ (m_1 - 2) + N_2\ (m_2 - 2)] \ln (c - 1)$$
$$- [N_1\ (m_1 - 1) + N_2\ (m_2 - 1)] \ln M \quad (18)$$

Relations similar to the mobile model arise for the fugacity and spreading pressure of the immobile model.

$$\ln f_j = -\partial \ln Q_i/\partial N_j - \mu_j^o(T)/(kT) \quad (19)$$

$$\pi/(kT) = \partial \ln Q_i/\partial A = (1/a)\ \partial \ln Q_i/\partial M \quad (20)$$

Adsorptive Energy

From Equations (16), (17), (18), and (19) the fugacities of the two components are

$$(\ln f_1)_i = \ln N_1 - m_1 \ln (M - m_1\ N_1 - m_2\ N_2) + (m_1 - 1) \ln M$$
$$- \{E_{i,1}(\theta_i) + (m_1/M)\ [N_1\ E'_{i,1}(\theta_i) + N_2\ E'_{i,2}(\theta_i)]\}/(kT)$$
$$- \ln j_{i,1} - \mu_1^o(T)/(kT) + (m_1 - 2) \ln (c - 1) + \ln c \quad (21)$$

$$(\ln f_2)_i = \ln N_2 - m_2 \ln (M - m_1\ N_1 - m_2\ N_2) + (m_2 - 1) \ln M$$
$$- \{E_{i,2}(\theta_i) + (m_2/M)\ [N_1\ E'_{i,1}(\theta_i) + N_2\ E'_{i,2}(\theta_i)]\}/(kT)$$
$$- \ln j_{i,2} - \mu_2^o(T)/(kT) + (m_2 - 2)\ln(c - 1) + \ln c \quad (22)$$

The arbitrary isothermal, composition independent, function only of coverage for the immobile model is defined as

$$\xi_i(\theta_i) \equiv \ln (f_1/N_1) - (m_1/m_2) \ln (f_2/N_2)$$
$$= [(m_1/m_2)\ E_{i,2}(\theta_i) - E_{i,1}(\theta_i)]/(kT) + C_6 \quad (23)$$

The ratio (m_1/m_2) and the function $\xi_i(\theta_i)$ are determined experimentally in the same manner as described for the mobile case.

In a similar fashion Equations (21) and (22) for pure component adsorption at a constant coverage lead to

$$\phi_i(\theta_i) \equiv \ln (f_1^o/N_1^o) - \ln (f_2^o/N_2^o)$$
$$= (m_2 - m_1) \ln (1 - \theta_i)$$
$$+ [E_{i,2}(\theta_i) - E_{i,1}(\theta_i)]/(kT)$$
$$+ \theta_i\ [E'_{i,2}(\theta_i) - E'_{i,1}(\theta_i)]/(kT) + C_7 \quad (24)$$

Again

$$\psi_i(\theta_i) = (1/\theta_i) \int [\phi_i(\theta_i) - C_7]\ d\theta_i \quad (25)$$

The solutions for the adsorptive energies are

$$E_{i,1}(\theta_i)/(kT) = [m_1\ \psi_i(\theta_i) - m_2\ \xi_i(\theta_i) + m_2\ C_8]/(m_2 - m_1) \quad (26)$$

$$E_{i,2}(\theta_i)/(kT) = [\psi_i(\theta_i) - \xi_i(\theta_i) + C_8]m_2/(m_2 - m_1) \quad (27)$$

Correlation

Essentially the same correlations as for the mobile model result for the immobile model

$$[\ln (f_1/N_1) - \ln (f_1^o/N_1^o)]_i = -(m_2/M)\ N_2\ \xi'_i(\theta_i) \quad (28)$$

$$= -(m_2/m_1)\ (N_2/A)\ \Xi'_i(N_i^*/A) \quad (28a)$$

$$[\ln (f_2/N_2) - \ln (f_2^o/N_2^o)]_i = +(m_2/M)\ N_1\ \xi'_i(\theta_i) \quad (29)$$

$$= +(m_2/m_1)\ (N_1/A)\ \Xi'_i(N_i^*/A) \quad (29a)$$

using the definitions

$$N_i^* = N_1 + (m_2/m_1)\ N_2 = (M/m_1)\ \theta_i \quad (30)$$

$$\Xi_i(N_i^*/A) = \xi_i(\theta_i) \quad (31)$$

SPREADING PRESSURE EXPRESSIONS FOR BOTH MODELS

Expressions for the spreading pressure are obtained from Equations (1), (2), (4), (16), (17), and (20); and from the energy functions, Equations (10), (11), (26), and (27).

$$[A\pi/(kT)]_m = (N_1 + N_2) + [b_2/(b_2 - b_1)]\ (N_1 + N_2)\ \theta_m\ \xi'_m(\theta_m) - [1/(b_2 - b_1)]\ (\theta_m)^2\ \psi'_m(\theta_m) \quad (32)$$

$$[A\pi/(kT)]_i = -M\ [\theta_i + \ln (1 - \theta_i)] + (N_1 + N_2) + [m_2/(m_2 - m_1)]\ \theta_i\ \xi'_i(\theta_i) - [1/(m_2 - m_1)]\ (\theta_i)^2\ \psi'_i(\theta_i) \quad (33)$$

Alternate expressions in terms of N^* in place of θ are

$$[A\pi/(kT)]_m = (N_1 + N_2) + [b_2/(b_2 - b_1)]\ (N_1 + N_2)\ (N_m^*/A)\ \Xi'_m(N_m^*/A) - [b_1/(b_2 - b_1)] \int (N_m^*/A)\ \Phi'_m(N_m^*/A)\ d(N_m^*/A) \quad (32a)$$

$$[A\pi/(kT)]_i = -[m_1\ N_i^* + M \ln (1 - m_1\ N_i^*/M)] + (N_1 + N_2) + [m_2/(m_2 - m_1)]\ (N_1 + N_2)\ (N_i^*/A)\ \Xi'_i(N_i^*/A) - [m_1/(m_2 - m_1)] \int (N_i^*/A)\ \Phi'_i(N_i^*/A)\ d(N_i^*/A) \quad (33a)$$

using the definitions

$$\Phi_m(N_m^*/A) = \phi_m(\theta_m) \quad (34)$$

$$\Phi_i(N_i^*/A) = \phi_i(\theta_i) \quad (35)$$

DISCUSSION

Fit of Experimental System to Correlations

Extensive experimental data (9) on the methane-ethane-silica gel system were used to evaluate the correlations presented above. Eight mixtures from pure methane to pure ethane, whose compositions are listed in Table 1, were used. The average value of the adsorptive energy and the absolute adsorption as measured experimentally (9) were used for the correlation study.

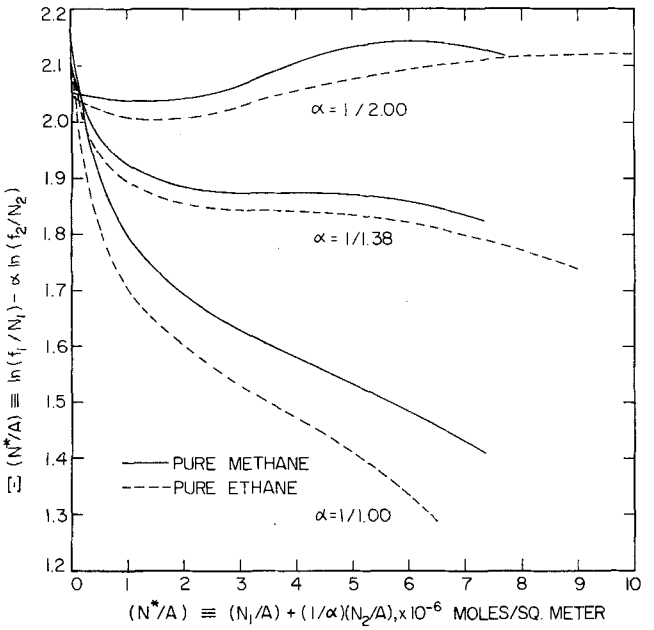

Fig. 1. Plots of Function $\Xi(N^*/A)$ vs. (N^*/A) for some choices of fitting constant α $(=b_1/b_2$ or $m_1/m_2)$, methane-ethane adsorption on silica gel at 25°C.

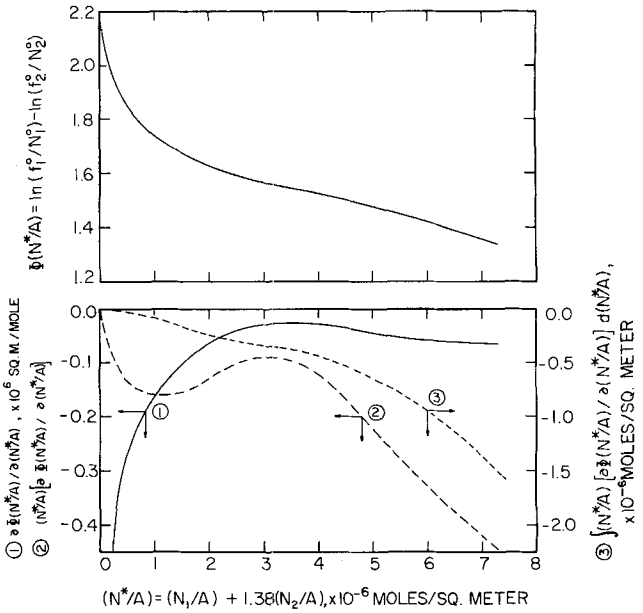

Fig. 3. Function $\Phi(N^*/A)$ and its derivatives as functions of (N^*/A) for methane-ethane adsorption on silica gel at 25°C.

TABLE 1. COMPOSITIONS OF GAS MIXTURES

Mixture	#1	#2	#3	#4	#5	#6	#7	#8
Methane	99.98	98.56	94.27	89.42	79.49	60.07	33.60	0.00
Ethane	0.02	1.44	5.58	10.58	20.51	39.79	66.40	99.94
air & others	—	—	0.15	—	—	0.14	—	0.06

The effect of varying the fitting ratio

$$\alpha = b_1/b_2 \quad \text{or} \quad m_1/m_2$$

was found by plotting the experimental fugacity groups versus the coverage θ, as given by Equations (7) or (23), for an isotherm. Some typical examples are given in Figure 1 for compositions number 1 and 8 at 25°C. As α varies from 1.0 to 0.5, the set of curves approach each other and converge and then begin to pull apart. Values of α for which the best convergence was obtained at the four temperatures are given in Table 2. The root-mean-square deviation at each temperature for all compositions from the average curve, $\Xi(N^*/A)$, is also given. Figure 2 shows the results at 25°C. for the average curve $\Xi(N^*/A)$ and its derivatives as functions of (N^*/A) using the best value of $\alpha = 1/1.38$.

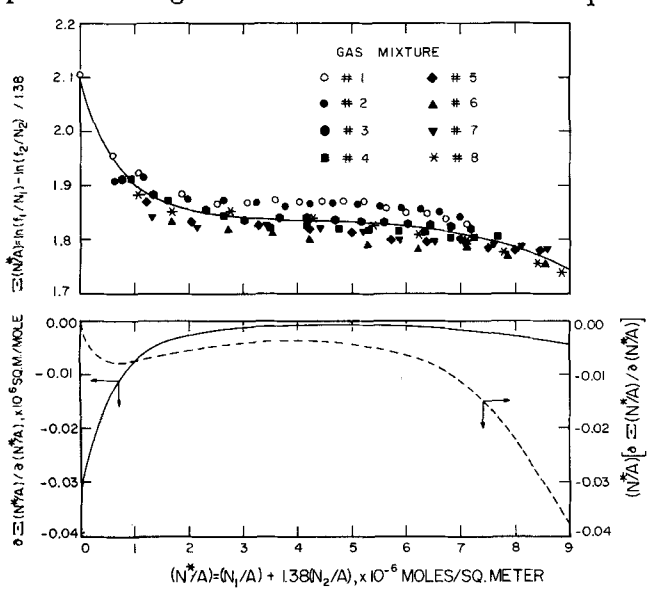

Fig. 2. Best fit for Function $\Xi(N^*/A)$ vs. (N^*/A) at $\alpha = 1/1.38$ and the derivatives, $\partial\Xi(N^*/A)/\partial(N^*/A)$ and $(N^*/A)[\partial\Xi(N^*/A)/\partial(N^*/A)]$, as functions of (N^*/A) for methane-ethane mixtures adsorption on silica gel at 25°C.

The pure component case, defined by the empirical function in Equation (8), converted to the same basis (N^*/A) by Equations (34) or (35), gives the results shown in Figure 3.

TABLE 2. FITTING CONSTANT α FOR BEST CONVERGENCE OF $\Xi(N^*/A)$ AND ROOT-MEAN SQUARE DEVIATION

Temperature, °C.	5.00	15.00	25.00	35.00
$\alpha = b_1/b_2$ or m_1/m_2	1/1.34	1/1.36	1/1.38	1/1.40
$\sqrt{\delta^2[\Xi'(N^*/A)]}$	0.0260	0.0250	0.0202	0.0213

Other ratios for comparison; methane-ethane system

	ratio
Two-dimensional van der Waals b	1/1.34
Gas phase van der Waals b	1/1.49
Square of collision diameter	1/1.33
Cube of collision diameter	1/1.55

Observed vs. Calculated Fugacity

The correlations given in Equations (12a) and (13a) were used to calculate the fugacities f_1 and f_2 for varying amounts of adsorption, N_1 and N_2. Figure 4 gives the results at 25°C. as the ratio of the calculated to observed fugacity as a function of (N^*/A). The ratio is always 1.00 ± 0.08. The methane fugacity ratio deviates slightly above 1.00; the resulting root-mean-square deviations for both methane and ethane are given in Table 3. The correlations given in Equations (12a) and (13a) are satisfactory, since the entire composition range and coverage from zero to about monolayer on the heterogeneous adsorbent are

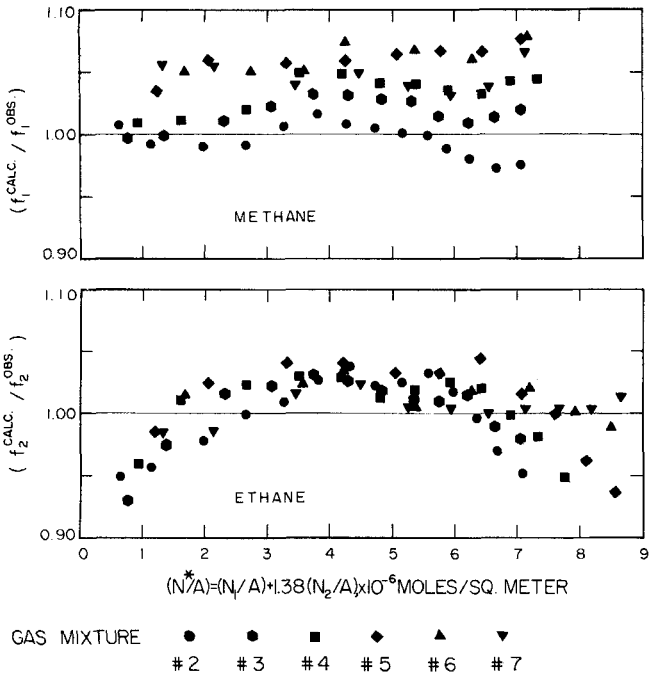

Fig. 4. Deviation of calculated fugacities from observed ones as functions of (N^*/A) for methane-ethane mixtures adsorption on silica gel at 25°C.

accounted for by one fitting constant within the deviation given above.

Figure 5 shows constant fugacity lines on the (N_1/A) — (N_2/A) plane as calculated from Equations (12*a*) and (13*a*) or from Equations (28*a*) and (29*a*). The terminal points on the boundaries $(N_1/A) = 0$ and $(N_2/A) = 0$ were based on the data for pure component adsorption which was used in Equations (12*a*) and (13*a*). Even if mixture data are not available, the pure gas and infinite dilution adsorption data suffice for the determination of

TABLE 3. FUGACITY ROOT-MEAN-SQUARE DEVIATIONS

Temperature, °C.	5.00	15.00	25.00	35.00
$\sqrt{\delta^2 (f_1^{cal}/f_1^{obs})}$	5.2%	4.1%	4.1%	4.3%
$\sqrt{\delta^2 (f_2^{cal}/f_2^{obs})}$	3.4%	2.7%	2.7%	2.9%

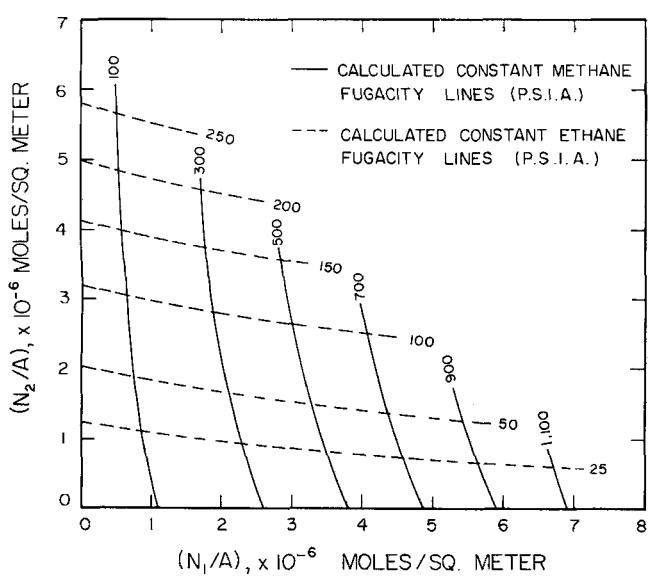

Fig. 5. Calculated constant fugacity lines on amounts of adsorption per unit area plane, (N_1/A) — (N_2/A), for methane-ethane mixtures adsorption on silica gel at 25°C.

the fitting constant α and the functions, $\Xi(N^*/A)$ and $\Phi(N^*/A)$. A specific combination of gases and adsorbent at a temperature give unique values for α, $\Xi(N^*/A)$, and $\Phi(N^*/A)$.

Observed vs. Calculated Spreading Pressure

The observed (*10*) and calculated spreading pressures for methane and ethane are shown in Figures 6 and 7. The ordinate is on the basis of the number of molecules per unit area. Two values were tried for the thickness of the adsorbed phase on the adsorbent. Previous calculations (*8, 9*) used 8.0 Å.; these calculations were made for both 6.0 and 8.0 Å. For the immobile model calculations, m_1 in Equation (33*a*) was assumed to be 1.0. The total number of adsorption sites per unit area, (M/A), was taken as 10×10^{-6} mole/sq. meter which is a realistic value for a molecule of 16.7 Å.^{2}. If $(M/A) = 20 \times 10^{-6}$ is used, the curve for the immobile model is closer to the curve for the mobile model.

For an adsorbed phase thickness $h = 8.0$ Å., the observed spreading pressure for methane adsorption lies below the region bounded by the curves for mobile and immobile models. For $h = 6.0$ Å., however, the observed values fall very close to the curve for the completely mobile model. The use of 6.0 Å., which is two times the collision diameter of the methane molecule, for h implies about 8.0 Å. from the cores of the surface atoms of the adsorbent. We conclude that methane adsorption has a thickness of 6.0 Å. and is a highly mobile type at ambient temperatures.

For either assumed adsorbed phase thickness, the observed spreading pressure for ethane adsorption falls in the region bounded by the mobile and immobile models. The larger value of h placed the observed points closer to the curve for the mobile model, which is reasonable since the mobility of molecules is greater at greater distances from the surface of the adsorbent and the average mobility for the adsorbed phase becomes larger for the larger h. Ethane adsorption on silica gel is concluded to be a mobile type, but less mobile than methane adsorption, at ambient temperatures. This conclusion is in good agreement with previous results (*8*) on adsorbed volume per molecule for silica gel adsorption.

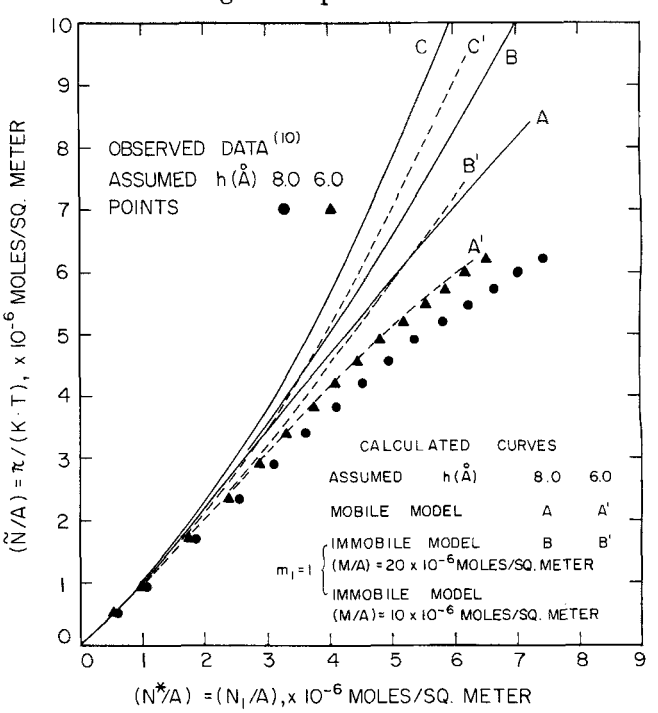

Fig. 6. Observed and calculated spreading pressures vs. (N^*/A) for methane adsorption on silica gel at 25°C.

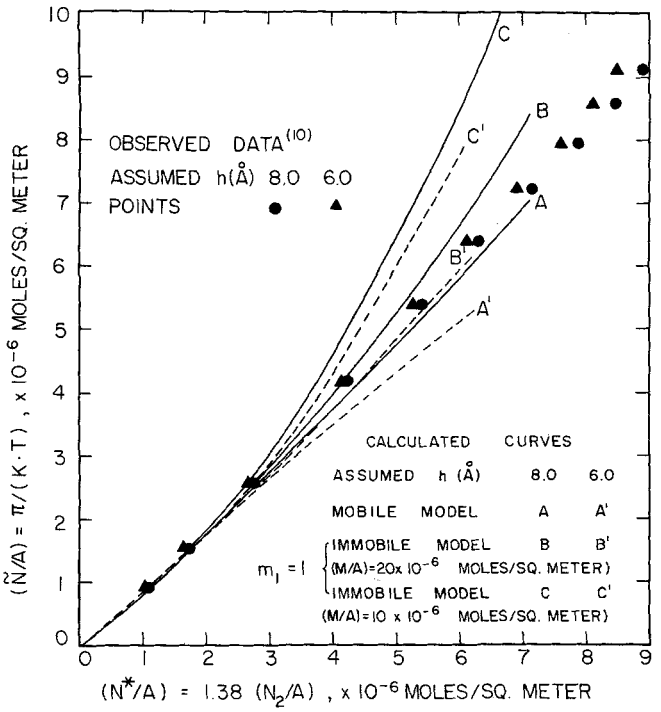

Fig. 7. Observed and calculated spreading pressures vs. (N^*/A) for ethane adsorption on silica gel at 25°C.

Comparison of Spreading Pressure to Macroscopic Gas Phase Pressure

Pressure in the macroscopic gas phase is directly related to the total molecular density by the ideal gas law with a nonideality factor z, the compressibility factor. Similar more complex expressions in the adsorbed phase for spreading pressure as a function of the amount of adsorption are given in Equations (32a) and (33a) for the mobile and immobile models. A simple plot of $\pi/(kT)$ vs. the total amount of adsorption per unit area, $\Sigma(N_j/A)$, gives different curves for several gas compositions. However, a trial plot of $\pi/(kT)$ vs. a weighted summation on a methane basis, $(N^*/A) = [N_1 + (1/\alpha)\, N_2]/A$, gives quite a small scattering of points with respect to gas composition and results in an almost straight line, as shown in Figure 8. A similar result with a different slope is obtained using a weighted sum on an ethane basis for the abscissa. The point of interest is the convergence of different gas compositions to form a single line at a constant $\alpha = 1/1.38$ which was determined by a fitting process of Equation (7) or (23) to the experimental data. The deviation of the plots from linearity may correspond to the compressibility factor for the macroscopic gas phase. The fitting constant, α, originally a ratio of the molecular sizes, is also useful as a factor relating the effect of the molecular species on the gas-solid interface energy ($A\pi$) on adsorption.

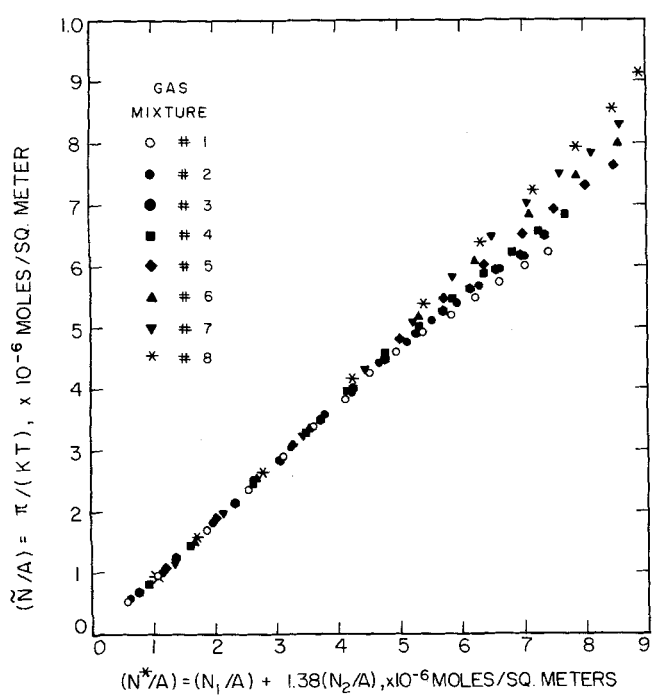

Fig. 8. Spreading pressure vs. weighted summation of absolute amount of adsorption per unit area on methane basis, $(N^*/A) \equiv (N_1/A) + (1/\alpha)(N_2/A)$, giving a good coincidence of curves for different gas compositions and forming an almost straight line; at 25°C.

CONCLUSIONS

The adsorption of a binary gas mixture on a heterogeneous adsorbent has been correlated for both mobile and immobile models. The form for both models was essentially equivalent. The required experimental data are on both pure components and on infinite dilution, which determines one fitting constant and an empirical function to describe the nonideality of the gas-solid interaction. The correlations satisfactorily describe the methane-ethane-silica gel system at ambient temperatures up to about monolayer adsorption.

Different expressions of the spreading pressure of the adsorbed phase were obtained for the mobile and immobile models. Based on a comparison of observed values to calculated spreading pressures, the system was classified as a highly mobile type of adsorption at ambient temperatures.

ACKNOWLEDGMENT

The National Science Foundation provided support for this work.

NOTATION

- a = average area of a single adsorption site for immobile model
- A = total surface area of adsorbent
- b = volume occupied by a molecule of adsorbate for mobile model
- c = number of nearest neighbor adsorption sites for immobile model
- C_3-C_8 = constants at a temperature with respect to coverage, contain j, μ, m, c, and M terms
- $E(\theta)$ = average adsorptive energy for a species at the surface coverage θ
- f = fugacity
- h = height of adsorbed phase
- j = internal-rotational-vibrational-translational partition function of a single adsorbate molecule
- k = Boltzmann constant
- m = number of adsorption sites occupied by a molecule of adsorbate for immobile model
- M = total number of adsorption sites for immobile model
- N = number of molecules in the adsorbed phase
- N^* = weighted summation of the number of molecules adsorbed on a methane basis as defined by Equation (14) or (34)
- Q = total partition function of the adsorbates
- T = absolute temperature
- V = volume of the adsorbed phase
- w = number of ways of distributing molecules to the adsorption sites for immobile model

Greek Symbols

α = fitting ratio b_1/b_2 or m_1/m_2
δ = deviation
θ = coverage of the solid surface by adsorbates
μ = chemical potential
ξ = empirical function of θ defined by Equation (7) or (23) for binary mixtures
Ξ = same as ξ but as function of (N^*/A)
π = spreading pressure of the adsorbed phase
ϕ = empirical function of θ defined by Equation (8) or (24) for pure component
Φ = same as ϕ but as function of (N^*/A)
ψ = empirical function of θ defined by Equation (9) or (25)
Ψ = same as ψ but as function of (N^*/A)

Superscripts

o = pure component adsorption; standard state condition
$'$ = derivative of the function with respect to parameter within parentheses

Subscripts

i = immobile model
j, k = species
m = mobile model
1, 2 = methane, ethane

LITERATURE CITED

1. Flory, P. J., *J. Chem. Phys.*, **9**, 660 (1941); **10**, 51 (1942).
2. Halsey, G., and H. S. Taylor, *ibid.*, **15**, 624 (1947).
3. Hill, T. L., *ibid.*, **14**, 441 (1946).
4. *Ibid.*, **17**, 762 (1949).
5. Honig, J. M., *Ann. N. Y. Acad. Sci.*, **58**, 74 (1954).
6. ———, and E. L. Hill, *J. Phys. Chem.*, **22**, 851 (1956).
7. Hoory, S. E., and J. M. Prausnitz, *Surface Sci.*, **6**, 377 (1967).
8. Masukawa, S., and Riki Kobayashi, *J. Gas Chromatography*, **6**, 257 (1968).
9. ———, *J. Chem. Eng. Data*, **13**, 197 (1968).
10. Masukawa, S., and Riki Kobayashi, *in submission to AIChE J.*, to be published.
11. Ross, S., and J. P. Olivier, "On Physical Adsorption," John Wiley, New York (1964).
12. Sips, R., *J. Chem. Phys.*, **16**, 490 (1948).
13. Steele, W. A., *J. Phys. Chem.*, **67**, 2016 (1963).

Manuscript received September 11, 1967; paper accepted November 1, 1967.

Heat Transfer Coefficients and Circulation Rates for Thermosiphon Reboilers

P. R. BEAVER and G. A. HUGHMARK

Ethyl Corporation, Baton Rouge, Louisiana

Heat transfer coefficients and circulating data were obtained for a single tube thermosiphon reboiler operated under vacuum and at atmospheric pressure. The results are compared with existing correlations. An analysis is presented for local heat transfer coefficients in the single phase and two-phase regions.

Normal operation of vertical thermosiphon reboilers at atmospheric and higher pressure results in a two-phase region for more than one-half of the tube length with the remainder of the tube length required for essentially single-phase liquid heating. Under vacuum conditions, the liquid heating section may represent as much as 90% of the tube length. The relatively short two-phase region at subatmospheric conditions would be expected to result in a lower circulation rate than is obtained with the longer two-phase region at atmospheric and higher pressure conditions. Experimental heat transfer and circulating rate data at subatmospheric conditions are limited with the result that design methods must be extrapolated for these conditions.

This paper reports an experimental study of a single tube thermosiphon reboiler operated under vacuum and at atmospheric pressure. Heat transfer coefficients and circulating rate data were obtained and are analyzed to provide confidence in design methods for vacuum conditions.

EXPERIMENTAL EQUIPMENT AND PROCEDURE

Figure 1 shows a sketch of the equipment. The tube was 8 ft. long ¾ in. schedule 80 carbon steel pipe. Electrical heating was used to provide a known flux at point locations on the pipe. Four heaters were used to provide a maximum flux of 9,000 B.t.u./hr. sq. ft. The heaters were made of Nichrome wire of 0.41 ohms/ft. resistance and were wound with ceramic beads around the wire. Each wire was 26.33 ft. long. Total power output at 117 v. was 5,700 w. Powerstats were used to control the heat to the pipe.

Iron-constantan thermocouples were attached to the outside pipe wall at the ends of the 8 ft. section and at 1 ft. intervals along the pipe. Holes 0.05 in. deep were drilled in the pipe wall, and the thermocouple junctions were pressed into these holes. A traveling thermocouple passed downward through the pipe to obtain process temperatures corresponding to the 1 ft. intervals.

The orifice was 0.500 in. diam. in a run of pipe the same as the heated pipe to minimize the pressure drop. Water and ethylene glycol were used to calibrate the orifice. The orifice differential pressure was obtained with a manometer.